Using superlattice ordering to reduce the band gap of random (In,Ga)As/InP alloys to a target value via the inverse band structure approach

Paulo Piquini[*] and Alex Zunger

National Renewable Energy Laboratory, Golden, Colorado 80401, USA

Thermophotovoltaic (TPV) devices are intended to absorb photons from hot blackbody radiating objects, often requiring semiconductor absorbers with band gap of $\simeq 0.6$ eV. The random $In_xGa_{1-x}As$ alloy lattice matched ($x_{In}=0.53$) to a (001) InP substrate has a low-temperature band gap of 0.8 eV, about 0.2 eV too high for a TPV absorber. Bringing the band gap down by raising the In concentration induces strain with the substrate, leading to a two-dimensional (2D)→three-dimensional (3D) morphological transition occurring before band gaps suitable for TPV applications are achieved. We use the inverse band structure approach, based on a genetic algorithm and empirical pseudopotential calculations, to search for *lattice-matched* InAs/GaAs multiple-repeat unit structures with individual layer thicknesses lower than the critical thickness for a 2D→3D transition. Despite the fact that quantum confinement usually *increases* band gaps, we find a quantum superlattice structure with the required *reduced* gap (and a significant optical transition) that matches all target requirements. This is explained by the predominance of (potential-energy) level anticrossing effects over (kinetic) quantum confinement effects.

Thermophotovoltaic (TPV) materials convert thermal energy into electricity by absorbing electromagnetic radiation from blackbody sources and creating electron-hole pairs. Unlike ordinary photovoltaic (PV) materials which use sunlight as the source (temperature $\simeq 5400$ °C), TPV devices are intended to absorb radiation from sources with lower temperatures, usually ranging from 900 to 1500 °C, requiring semiconductor absorbing materials with energy band gaps in the range of 0.4–0.7 eV. Silicon and germanium were first tried as TPV converters but were eventually abandoned because of low efficiency below 1700 °C.[1] The increase in the quality of the available III-V semiconductor materials has recently renewed interest in TPV as an energy source. To achieve good quality (dislocation-free) *thick* absorber film, one needs the film to be lattice matched to a substrate. At the same time, TPV compatibility requires the absorber to have the desired target band-gap value and strong direct transition. The need to simultaneously satisfy such multiple materials constraints poses a serious challenge. Two materials groups have been studied: (i) InGaAsSb/GaSb (Ref. 2) and (ii) InGaAs/InP.[3] The quaternary $In_xGa_{1-x}As_ySb_{1-y}$ random alloy can be grown lattice matched to a GaSb substrate for a wide range of (x,y) compositions, delivering a band gap varying from 0.4 to 0.8 eV.[4] However, the GaSb substrate has a high absorption coefficient, which compromises its practical applicability due to the high power absorption, increasing the converter's temperature while not allowing the recycling of photons not absorbed by the converter. On the other hand, the pseudobinary $In_xGa_{1-x}As$ random alloy can be lattice matched to a given substrate only for a single film composition x. For example, $In_{0.53}Ga_{0.47}As$ is lattice matched to an InP substrate. Figure 1 shows the valence-band maximum (VBM) and the conduction-band minimum (CBM) of random $In_xGa_{1-x}As$ (a) as well as its band gap (b) as a function of the film In composition x, as obtained from a pseudopotential calculation described below. We see that at the lattice-matched composition $x_{In}=0.53$ (vertical dashed line) the low-temperature band gap is $E_g=0.82$ eV (0.74 eV at room

T), too high for the usual thermal sources requiring $E_g=0.6$ eV at low T. On the other hand, reducing the band-gap value to the desired target of $\simeq 0.6$ eV requires an $In_xGa_{1-x}As$ alloy with $x_{In} \simeq 0.84$ [empty square in Fig. 1(b)], leading to a large in-plane stress [Fig. 1(c)]. Indeed, the growth of highly strained $In_{0.84}Ga_{0.16}As$ random alloys directly on InP substrate leads to the appearance of a high concentration of misfit dislocations,[5,6] degrading the quality and reducing the efficiency of the converter.[7] The question posed here is: Is it possible to use atomic ordering (as opposed to randomness) to identify (InAs)/(GaAs) superlattices that are directly lattice matched to InP substrate and have a target band gap (of, e.g., 0.6 eV) with a significant allowed transition? The bold solid arrow in Fig. 1(b) shows the reduction needed in the band gap of random $In_{0.53}Ga_{0.47}As$ to achieve these conditions.

This is a challenging proposition for three reasons. First, quantum confinement present in (narrow) superlattices usually *raises* the band gap. We seek for a gap *reduction* whereby band-folding (potential-energy) effects would counteract (kinetic) confinement effects, making the search for such (quantum) effect nontrivial. Second, even though *any* (InAs)/(GaAs) superstructure with 53% In composition is lattice matched to InP as a whole (so the stress at the substrate interface vanishes), the large ($\simeq 7\%$) lattice mismatch between the InAs and GaAs constituents implies that the thicknesses of the individual $(InAs)_n$ and $(GaAs)_m$ layers must be kept below the critical thickness for two-dimensional (2D)→three-dimensional (3D) morphological transition. Calculations[8] and experiment[9] suggest critical thicknesses for the InAs and GaAs layers of around 5 monolayers (MLs). This places an additional constraint on this material search problem. Third, *single-repeat* unit structures[10] $(AC)_n/(BC)_m/(AC)_n/(BC)_m \cdots$, where the periods (n,m) are constant throughout and are closely lattice matched to InP, can achieve the target gap of $\simeq 0.6$ eV only for $n \approx 20$ MLs (Fig. 2), exceeding by far the critical thickness for individual (InAs) and (GaAs) layers on InP sub-
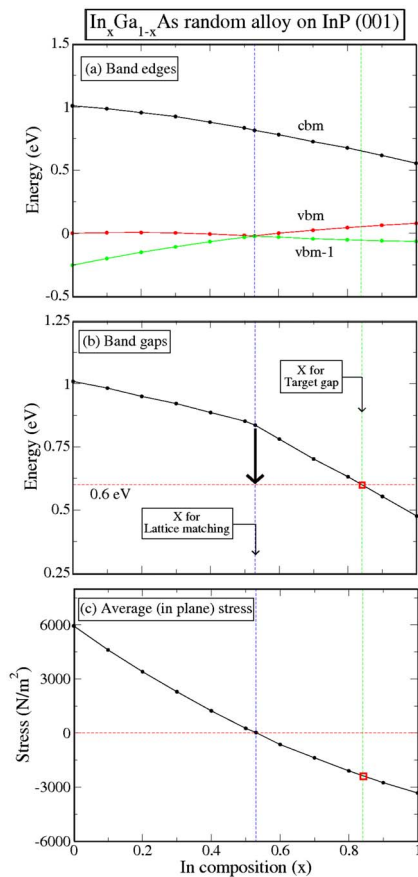
PAULO PIQUINI AND ALEX ZUNGER

FIG. 1. (Color online) Electronic properties of random $In_xGa_{1-x}As$ alloy as obtained by solving the pseudopotential plane-wave eigenvalue problem using a zinc-blende supercell with 512 atoms, where the Ga and In site occupations were determined by random statistics at composition x. (a) Band edges. The CBM, VBM, and VBM-1 labels refer to the conduction-band minimum, valence-band maximum, and the level immediately below the VBM in energy, respectively. (b) Band gaps. (c) Average in-plane stress. The vertical dashed lines indicate the $In_{0.53}Ga_{0.47}As$ composition lattice matching a InP substrate. The empty square in (c) indicates the in-plane stress of the $In_{0.84}Ga_{0.16}As$ random alloy that gives the target gap of 0.6 eV and is lattice matched to an InP substrate.

strates ($n \simeq 5$). One thus needs to consider a more complicated material search problem, allowing for multiple-repeat unit structures $(AC)_n/(BC)_m/(AC)_p/(BC)_q \cdots$. Thus, our problem can be articulated as a search for $(InAs)_n/(GaAs)_m/(InAs)_p/(GaAs)_q \cdots$ multiple-repeat units that: (i) have a target band gap of 0.6 eV (at low T), (ii) have an overall composition that warrants the lattice matching on an InP substrate (53% of In), and (iii) have individual InAs and GaAs layers not thicker than the critical thicknesses for the 2D→3D morphological transition (5 MLs). This exemplifies a class of design problems that cannot be addressed by *direct* computational strategies because of the complexity of the search space. The size of the configurational space available in our search is in principle 2^N, where N is the number of cation (In,Ga) sites in the unit cell. However, restrictions appear when we limit the thicknesses of the stacking InAs and GaAs layers to be lower or equal to 5 MLs. These kinds
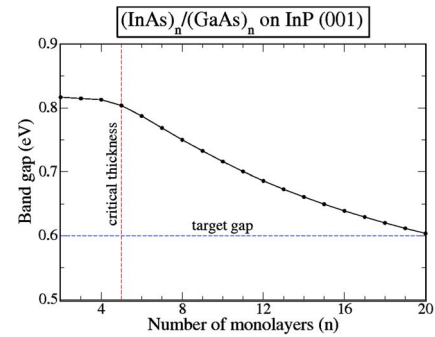

FIG. 2. (Color online) Band gaps for the (001) $(InAs)_n/(GaAs)_n$ ($n = 2, 20$) superlattices on a InP substrate, calculated using the empirical pseudopotential method. The vertical and horizontal dashed lines represent the critical thickness ($n \simeq 5$) and the IBS target band gap (0.6 eV), respectively.
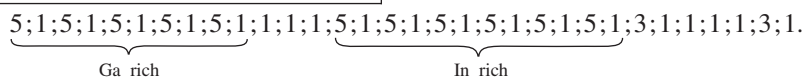
of problems can, on the other hand, be addressed by an inverse band structure (IBS) approach, searching for a configuration with the target material properties. Such a search in complex configurational spaces is efficiently performed by using evolutionary approaches that, unlike combinatorial chemistry, learn very fast from the initial steps, thereby requiring to visit only a tiny part of the whole configurational space. The IBS approach has been previously applied with success to predict the maximum band-gap configuration of the $Al_{0.25}Ga_{0.75}As$ superstructures,[11] to the design of nitrogen impurity in GaP (Ref. [12]) (to match targets such as minimum impurity-induced strain energy and lowest-energy valence-to-impurity optical transition), and to find the atomic configurations in GaInAsSb quaternary compounds, lattice matched to a GaSb substrate, that have a target band gap in the midinfrared wavelength region.[13] In all these cases, the available configurational spaces were enormous, turning practically impossible the use of *direct* methods.[14]

Method. Our search for the multiple-repeat unit structure has been performed using a supercell with $1 \times 1 \times 40$ conventional cubic cells along the (100), (010), and (001) directions, respectively, comprising a total of 320 atoms (80 monolayers). Each monolayer along the (001) direction is composed of either pure InAs or pure GaAs. A total of 42 InAs layers and 38 GaAs layers have been used in order to have an overall composition that is the closest to the one lattice matching the (001) InP substrate (53% In). The supercell basal plane is constrained to have the lattice parameter of the InP substrate (5.8687 Å). We start the genetic algorithm search[15] by creating a initial population of 60 independent individuals by randomly occupying the cation sites (layers) according to the overall composition $x_{In} = 0.53$. Once the population is set up we optimize the atomic positions and minimize the strain along the (001) direction using the valence force field method (VFF).[10,16] The fitness of each individual in the population, i.e., the departure of the electronic structure from the target properties, is then evaluated by solving the single-particle Schrödinger equation $\{\frac{\beta}{2}\nabla^2 + V_{ps}\}\psi_i(\mathbf{r}) = \epsilon_i\psi_i(\mathbf{r})$, where V_{ps} is the pseudopotential, which is written as a superposition of atomic screened pseudopotentials v_α of each atomic type α as $V_{ps} = \Sigma_{\alpha,n}v_\alpha(\mathbf{r} - \mathbf{R}_n - \mathbf{d}_\alpha)$, with d_α being the position vector of atom α (In,Ga or As)

relative to the unit-cell lattice vector R_n. The atomic pseudo-potentials have been fitted to reproduce calculated and measured properties of the InAs and GaAs binaries and the InGaAs pseudobinary.[10] The fitted properties are the band gaps and the eigenvalues close to the band edges at the Γ, L, and X points of the Brillouin zone, the effective masses, the deformation potentials, the spin-orbit splittings, and the band offsets. The parameter β appearing as a multiplicative factor to the kinetic energy recovers, to a first-order approximation, the self-energy contributions.[17] The wave functions $\psi_i(\mathbf{r})$ are expanded in a plane-wave basis and the eigenvalue problem is solved efficiently by the linear scaling folded spectrum method.[18]

The evolutionary search proceeds by generating offspring through crossover and mutation operations among the individuals in the current population. Crossover and mutation rates of 75% and 25%, respectively, have been used. The population evolves by replacing the 10 worst fitting individuals in the current population with the generated offspring. The search is stopped after 100 generations. Approximately 1050 band-gap evaluations are performed in each complete evolutionary search, corresponding to 60 evaluations at the initial generation plus 10 in each of the remaining ≈ 99 generations. A total of 20 independent runs have been performed. We imposed a constraint on the possible offspring configurations in order to keep the thickness of each individual InAs and GaAs layers lower than the transition thickness. This is done by discarding every generated offspring that has individual InAs or GaAs layers thicker than 5 MLs.

Results. Atomic structure: Figure 3 shows the evolution of the band gap for each of the 20 independent evolutionary runs along ≈ 100 generations. It shows that 65% of the runs lead to structures with band gaps within 0.01 eV from the 0.6 eV target value, with the other 35% giving band gaps between 6.03 eV and the target value. An analysis of the sequence of atomic layers along the (001) direction for each final IBS shows that the characteristic feature of the target IBS is an InAs-rich segment with $[(\mathrm{InAs})_5/(\mathrm{GaAs})_1]$ units. Also frequent is the presence of a GaAs-rich segment
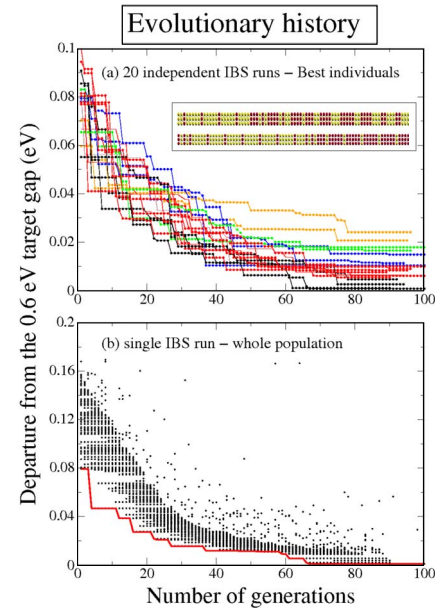

FIG. 3. (Color online) (a) Evolution of the band-gap values of the best individuals of the populations for the 20 independent IBS searches. Each IBS search runs along ≈ 100 genetic algorithm steps (generations) in the search for a 0.6 eV band-gap (InAs)/(GaAs) multiple-repeat structure, which is lattice matched to a (001) InP substrate. The inset shows the sequences of In and Ga atoms (As atoms are not shown) along the (001) direction for the IBS final structures with the best (bottom) and worst (top) matches to the target band gap, respectively. (b) Evolution of the band gaps of each individual in the population for the IBS search which gives the closest match (10^{-4} eV) to the 0.6 eV target gap.

with a number of $[(\mathrm{GaAs})_5/(\mathrm{InAs})_1]$ units. The best IBS configuration, with a band gap within 10^{-4} eV from the 0.6 eV target gap, has a $(n,m,p,q,\dots)$ sequence of $(\mathrm{GaAs})_n/(\mathrm{InAs})_m/(\mathrm{GaAs})_p/(\mathrm{InAs})_q\cdots$ layers given by [see inset of Fig. 3(a)]

$$\underbrace{5;1;5;1;5;1;5;1;5;1}_{\text{Ga rich}};1;1;1;\underbrace{5;1;5;1;5;1;5;1;5;1;5;1}_{\text{In rich}};3;1;1;1;1;3;1.$$

In general, these InAs-rich and GaAs-rich segments are separated by regions where the stacking sequence of (InAs) and (GaAs) layers has no specific pattern, and the thickness of the individual layers is mainly lower than 3. The inset of Fig. 3(a) shows the final structures with the closest (10^{-4} eV) and farthest (10^{-2} eV) band gaps with respect to the 0.6 eV target. The differences among the configurations appear: (i) in the degree of separation between the InAs-rich and GaAs-rich segments, and (ii) in the stacking sequence inside the InAs-rich and GaAs-rich segments. The greater the concentrations of In and Ga atoms in the InAs- and GaAs-rich segments, respectively, and the more closely the $[(\mathrm{InAs})_5/(\mathrm{GaAs})_1]$ and the $[(\mathrm{GaAs})_5/(\mathrm{InAs})_1]$ units patterns are followed inside the InAs-rich and GaAs-rich segments,

respectively, the greater will be the reduction and the closer to the target the band gaps will be. The InAs-rich segment is more clearly defined in the structures, with the GaAs-rich segment showing more variability in its composition and pattern. Figure 3(b) shows the evolution of the whole population along the evolutionary search with the best final match to the target band gap. It shows that the variability in the population is abruptly reduced around the step number 90.

Electronic structure: That this sequence can satisfy our target electronic structure is totally unsuspected and unpredictable in advance. Yet, after the fact we can inspect this structure and gain some insight into its main motifs. Figures 4(a) and 4(b) show the squared wave functions associated with the valence-band maximum and conduction-band mini-

mum of the structure shown in Fig. 4(c) along the (001) direction. It can be seen that both wave functions present the greatest contributions in the InAs-rich segment of the multiple-repeat structure, resulting in a spatially direct band gap. The CBM spreads along all of the InAs-rich segment, while the VBM is more concentrated in the middle part of the InAs-rich segment. As Fig. 4(d) shows, the GaAs-rich region constitutes a barrier for both electrons and holes, as it should be expected. The whole band-offset profile shows a type-I-like character, with electron and holes effectively confined in the InAs-rich segment. The thin GaAs monolayers in between InAs-rich segments play the role of strain relievers in the InAs-rich segments and have small influence on the intensities of the CBM and VBM squared wave functions, as can be seen in Figs. 4(a) and 4(b). The same role is played by the thin InAs layers in the GaAs-rich part of the structure. Thus, the intercalation of thin GaAs and InAs layers in the InAs-rich and GaAs-rich segments, respectively, reduce the internal strain between the stacking layers of the super-lattice while keeping an effective type-I band offset, reducing the band gap to a 0.6 eV target gap. The calculated dipole matrix element square for the VBM→CBM transition in the best-matched structure shown in Fig. 4(c) is significant, with the transition probability being around 30% of that for the bulk GaAs. Different from the bulk, there is a difference in intensity between the transitions with parallel and perpendicular polarizations. The transitions with perpendicular polarizations ($\langle 110 \rangle$ directions) are 10^2 times stronger than that for parallel (001) polarization. This should be expected once both VBM and CBM levels are concentrated in the InAs-rich layers, which reduces the probability of transitions between InAs and GaAs along the (001) growth direction.

In conclusion, we applied the IBS method in the search for (InAs)/(GaAs) structures that lattice match to a (001) InP substrate and have a target band gap of 0.6 eV. We found that a complex multiple-repeat unit satisfies the requirements imposed by the target band gap and the critical thickness of the individual InAs and GaAs layers. The final IBS structure has a spatially direct band gap and a significant VBM→CBM dipole matrix element square.
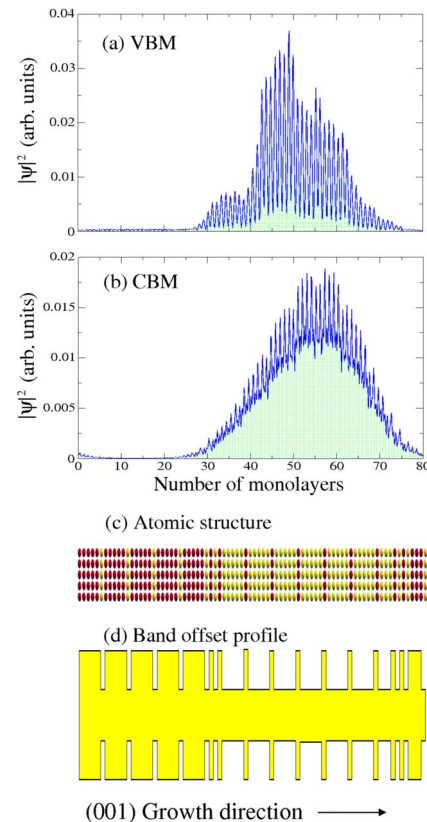

FIG. 4. (Color online) Squared wave functions of the (a) VBM and (b) CBM for the final IBS structure, shown in (c), where the red and blue circles represent Ga and In atoms (As is not shown), respectively. The band offset profile of this final IBS structure is shown in (d).

*Permanent address: Departamento de Física, Universidade Federal de Santa Maria, 97105-900, Santa Maria, RS, Brazil.

[1] B. Bitnar, Semicond. Sci. Technol. **18**, S221 (2003).

[2] M. W. Dashiell *et al.*, IEEE Trans. Electron Devices **53**, 2879 (2006).

[3] C. Rohr *et al.*, J. Appl. Phys. **100**, 114510 (2006).

[4] R. Magri *et al.*, J. Appl. Phys. **98**, 043701 (2005).

[5] T. Yagi *et al.*, Jpn. J. Appl. Phys., Part 2 **22**, L467 (1983).

[6] S. Lee *et al.*, Int. J. Solids Struct. **45**, 746 (2008).

[7] It is possible to grow mismatched In$_x$Ga$_{1-x}$As on InP by first growing a buffer layer of InAs$_y$P$_{1-y}$ alloy, in which the As concentration in the buffer changes from small values near the interface with InP, growing to a concentration that makes it lattice matched to the InGaAs converter. The misfit dislocations occur at the InAsP/InP interface, away from the InGaAs region. Although the InAsP buffer layer can reduce the number of dislocations in the InGaAs TPV converter, the efficiency of the TPV converter would approach its maximum performance if one could grow thick, good quality InGaAs samples on InP substrates and absorbing at the wavelength region of interest for TPV purposes.

[8] A. Sasaki *et al.*, Thin Solid Films **367**, 277 (2000).

[9] D. K. Oh *et al.*, J. Electron. Mater. **25**, 485 (1996).

[10] K. Kim *et al.*, Phys. Rev. B **66**, 045208 (2002).

[11] A. Franceschetti and A. Zunger, Nature (London) **402**, 60 (1999).

[12] S. V. Dudiy and A. Zunger, Phys. Rev. Lett. **97**, 046401 (2006).

[13] P. Piquini *et al.*, Phys. Rev. Lett. **100**, 186403 (2008).

[14] P. Piquini *et al.*, Phys. Rev. B **77**, 115314 (2008).

[15] K. Kim *et al.*, J. Comput. Phys. **208**, 735 (2005).

[16] P. N. Keating, Phys. Rev. **145**, 637 (1966).

[17] H. Hedin, J. Phys.: Condens. Matter **11**, R489 (1999).

[18] L. W. Wang and A. Zunger, J. Chem. Phys. **100**, 2394 (1994).